

Three-Dimensional Imaging of Strain in a Single ZnO Nanorod

Marcus C. Newton, Steven J. Leake, Ross Harder, and Ian K. Robinson

(Dated: November 27, 2009)

I. SUMMARY OF RESULTS

In this letter we show how advances in our fabrication techniques and experimental methods have allowed diffraction patterns to be obtained from multiple Bragg reflections of same nanocrystal for the first time. All three components of the ion displacement field and in turn, all six independent components of the strain tensor have been imaged in three dimensions using six Bragg reflections.

II. ARBITRARY PHASE OFFSET FOR A RECONSTRUCTED DATASET

When reconstructing the phase of an object using iterative projective algorithms, we specify a real-space phase range ($\phi_{c_{min}} < \phi_i < \phi_{c_{max}}$) constraint for which the reconstructed phase must reside within. If the reconstructed phase range of the data ($\phi_{r_{min}}, \phi_{r_{max}}$) is smaller than (rather than equal to) the phase range constraint, phase values can deviate uniformly by a maximum amount $\phi_{0_{max}}$.

$$\phi_{0_{max}} = (\phi_{c_{max}} - \phi_{c_{min}}) - (\phi_{r_{max}} - \phi_{r_{min}}) \quad (\text{S1})$$

This results in an arbitrary offset because there is no absolute phase origin of the diffraction. Because the different images used to construct the displacement field can have different offsets, we fix them through the following requirement:

$$\sum_i \rho_i (\phi_i - \phi_0) = 0 \quad (\text{S2})$$

\Rightarrow

$$\phi_0 = \frac{\sum_i \rho_i \phi_i}{\sum_i \rho_i} \quad (\text{S3})$$

where the sum is taken over all voxels i and ρ_i is the amplitude of the complex image density at voxel i .

III. DISPLACEMENT FIELD RECONSTRUCTION FOR THE OVERDETERMINED CASE OF $n > 3$

For every voxel in the image there are n phases corresponding to the n momentum transfer vectors (Bragg peaks) measured. $n = 2$ or 6 for the examples discussed in this paper. The following evaluation of the displacement field is carried out separately for every voxel.

The phase ϕ_i is related to the displacement u_j by:

$$\phi_i = q_{ij}u_j \quad (\text{S4})$$

where q_{ij} is the matrix formed by the $i \in \mathbb{N}_1$ momentum transfer vectors. The index j in u_j represents the $\{x, y, z\}$ components in a rectilinear coordinate frame. In general, we can obtain the displacement vector as follows:

$$u_j = q^{ij}\phi_i; \quad q^{ij}q_{ij} = \delta_j^i \quad (\text{S5})$$

We note that $q^{ij} = (q_{ij})^{-1}$ is the inverse matrix (with units of length). Now, q_{ij} is in general not a square matrix. When $n > 3$, a regressive approach is necessary (Treated here). A special case occurs for $n = 3$ where we can in general directly invert the matrix. When $n = 2$ we must rotate the co-ordinate system to reduce the shape of the matrix from $(2, 3)$ to $(2, 2)$ (See Below).

In the present case, the matrix q_{ij} (equation S4) is not a square matrix and hence has no well defined inverse. We therefore apply a regressive approach based on the “method of least squares” to obtain the displacement vector components. In this approach we minimise the sum of squares of residual $S \equiv \sum_i r_i r_i$; $r_i = q_{ij}u_j - \phi_i$ such that:

$$\frac{\partial S}{\partial r_i} \frac{\partial r_i}{\partial u_j} = 0 \quad (\text{S6})$$

from the definition:

$$\frac{\partial r_i}{\partial u_j} = q_{ij} \quad (\text{S7})$$

Substituting into equation S6:

$$\frac{\partial r_i^2}{\partial r_i} \frac{\partial r_i}{\partial u_j} = 2r_i q_{ij} = 2q_{ij}(q_{ik}u_k - \phi_i) = 0 \quad (\text{S8})$$

\Rightarrow

$$q_{ij}q_{ik}u_k - q_{ij}\phi_i = 0 \quad (\text{S9})$$

Rearranging we have:

$$u_i = \xi_{ij} q_{kj} \phi_k ; \quad \xi_{ij} = (q_{ki} q_{kj})^{-1} \tag{S10}$$

where $(q_{ki} q_{kj})^{-1}$ is the inverse matrix of $q_{ki} q_{kj}$ (with units of square length).

IV. DISPLACEMENT FIELD RECONSTRUCTION FOR $n = 2$

Here we derive a method to deduce the displacement vector components in rectilinear coordinates for $n = 2$. We transform e_i to the coordinates e'_i as follows:

$$e'_3 = \hat{a}_i = (a_i^2)^{-2} a_j e_j ; \quad a_i = \epsilon_{ijk} q_{nj} q_{mk} \tag{S11}$$

$$e'_2 = \hat{q}_{1i} ; \quad \hat{q}_{1i} = (q_{1i}^2)^{-2} q_{1j} e_j \tag{S12}$$

$$e'_1 = (b_i^2)^{-2} b_j e_j ; \quad b_i = \epsilon_{ijk} e'_{3j} e'_{2k} \tag{S13}$$

Using equations S11, S12 and S13 we obtain a relationship of the form:

$$e'_i = f(q_{mn})_{ij} e_j \tag{S14}$$

and hence:

$$q'_{im} = f(q_{mn})^{ij} e_j \tag{S15}$$

We can then invert q'_{ij} (equation S15) for use in equation S4.

□

V. FIGURES

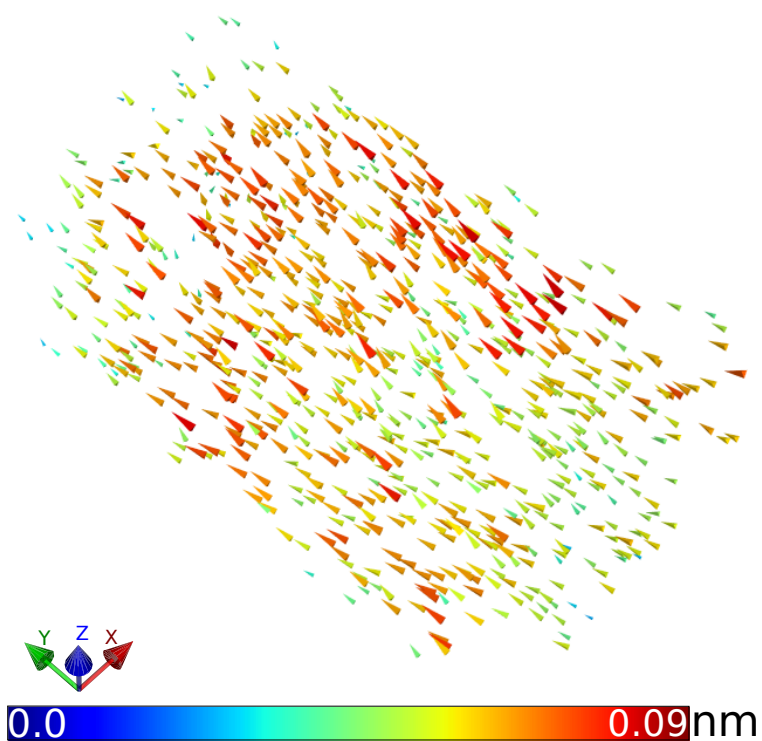


FIG. S1: Isosurface of the diffraction pattern of the measured amplitude (a) and the amplitude calculated from the reconstructed object (b) for each data set.

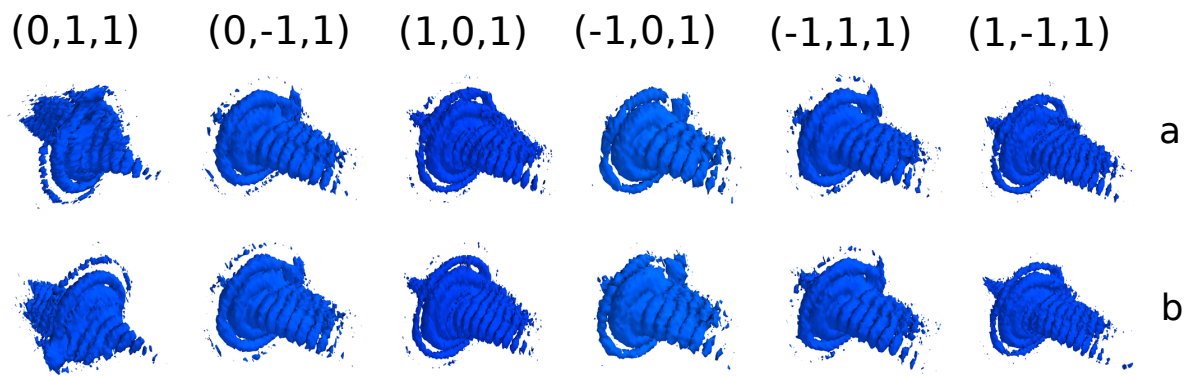


FIG. S2: Three-dimensional displacement field shown as arrows along the full length of the nanocrystal structure in iso-metric projection.

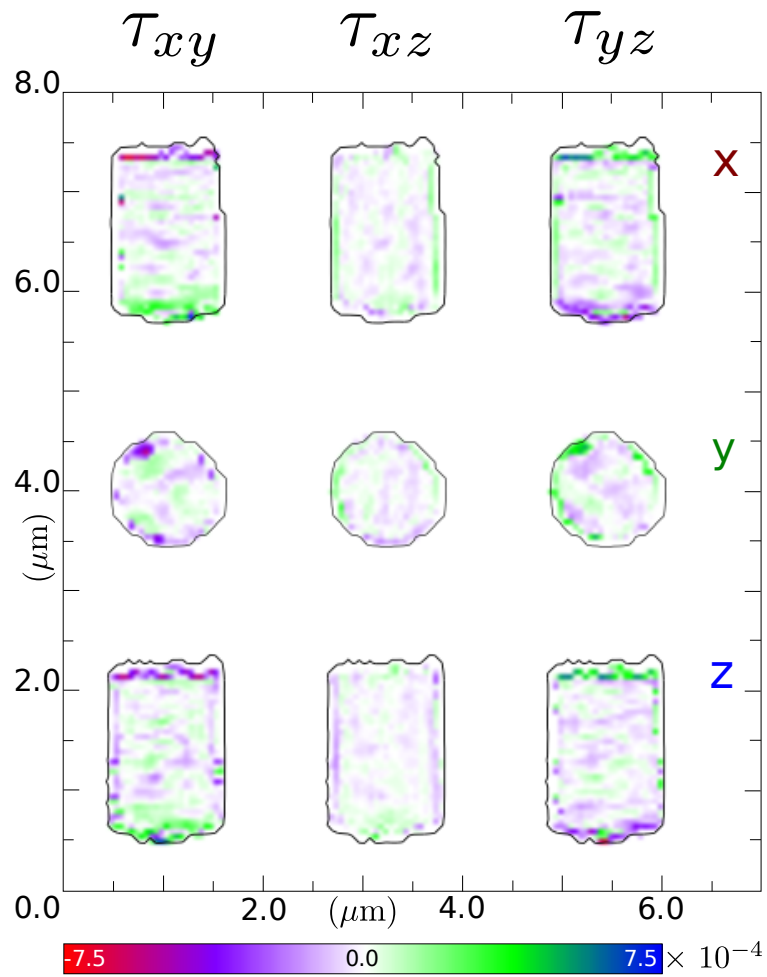


FIG. S3: Two-dimensional slices of all three unique components of the anti-symmetric rotation tensor taken along the three cartesian axis.